Mod Pathol 37 (2024) 100529

MODERN PATHOLOGY

USCAP UNITED STATES AND CANADIAN ACADEMY OF PATHOLOGY
Creating a Better Pathologist

Journal homepage: https://modernpathology.org/

Research Article

Age-Related Clusters and Favorable Immune Phenotypes in Young Breast Cancer Patients

Lise Martine Ingebriktsen[a], Amalie Abrahamsen Svanøe[a], Anna Kristine Myrmel Sæle[a,b], Rasmus Olai Collett Humlevik[a], Karen Toska[c], May Britt Kalvenes[a], Turid Aas[d], Anette Heie[d], Cecilie Askeland[a,b], Gøril Knutsvik[a,b], Ingunn Marie Stefansson[a,b], Lars Andreas Akslen[a,b], Erling Andre Hoivik[a,b], Elisabeth Wik[a,b,*]

[a] *Centre for Cancer Biomarkers CCBIO, Section for Pathology, Department of Clinical Medicine, University of Bergen, Norway;* [b] *Department of Pathology, Haukeland University Hospital, Bergen, Norway;* [c] *Section for Cancer Genomics, Haukeland University Hospital, Bergen, Norway;* [d] *Department of Surgery, Section for Breast and Endocrine Surgery, Haukeland University Hospital, Bergen, Norway*

ARTICLE INFO

Article history:
Received 3 November 2023
Revised 12 May 2024
Accepted 21 May 2024
Available online 27 May 2024

Keywords:
breast cancer
breast cancer in young
tumor microenvironment
gene expression

ABSTRACT

Breast cancer (BC) patients aged <40 years at diagnosis experience aggressive disease and poorer survival compared with women diagnosed with BC at 40 to 49 years, but the age-related biology is described to little extent. Here, we explored transcriptional alterations in BC to gain better understanding of age-related tumor biology. We studied a subset of the Bergen in-house cohort (n = 127; age range, 26-49 years) and used the NanoString Breast Cancer 360 expression panel on formalin-fixed paraffin-embedded BC tissue, and publicly available global BC messenger RNA expression data (n = 204; age range, 22-49 years), to explore differentially expressed genes between the young (age <40 years) and older (age 40-49 years) patients. Unsupervised hierarchical clustering was applied to identify gene expression–based patient clusters. We applied established computational approaches to define the PAM50 subtypes, risk of recurrence scores (ROR), and risk groups and to infer the proportions of 22 immune cell types from bulk gene expression profiles of patients aged <50 years at BC diagnosis. Differentially expressed genes and gene sets were investigated using OncoEnrichR and g:Profiler to describe functional profiles and pathway enrichment. We identified 4 age-related patient clusters presenting distinct characteristics of PAM50 subtypes and ROR profiles, which demonstrated independent prognostic value when adjusted for traditional clinicopathologic variables and the known molecular subtypes. Our findings showed better survival than expected in the basal-enriched cluster 2 and in triple-negative and basal-like BC. Deconvolution analyses of immunophenotypes indicated higher levels of M0 and M1 macrophages than M2 macrophages in subsets of young BC. Our approach identifies age-based patient clusters with distinct clinicopathologic profiles, to a large extent overlapping with the PAM50 subtypes, although with independent prognostic values in multivariate survival analyses. The patient clusters provided new insight in the immune cell distribution across tumor subtypes, potentially contributing to survival differences between the clusters and the molecular subtypes and indicating age-related mechanisms improving outcome. Our study confirms the applicability of ROR as a valid prognosticator also in a young BC cohort.

These authors contributed equally: Erling Andre Hoivik and Elisabeth Wik.

* Corresponding author.
E-mail address: Elisabeth.wik@uib.no (E. Wik).

https://doi.org/10.1016/j.modpat.2024.100529

Introduction

Breast cancer (BC) has surpassed lung cancer as the most frequent diagnosed cancer worldwide and is accountable for 11.7 % of all cancer incidents globally.[1]BC in young women, often defined as women aged <40 years at diagnosis, concerns a patient group that experiences more aggressive disease and poorer survival compared with women diagnosed with BC at 40 to 49 years.[2-6] In the United States, around 11,000 young breast cancer patients are diagnosed annually, and BC is the leading cause of cancer deaths among younger women.[7] Moreover, in the United States and several European countries, it is reported a small but significant increase in annually new BC cases for women aged <35 and 40 years (1.2% and 2%, respectively).[8,9]

It has been demonstrated that young age is an independent risk factor for disease recurrence and death.[10] Moreover, accumulating studies suggests that biological and molecular differences explain the poor prognosis seen in the young.[3,11-14] Higher proliferation in the young than that in older BC patients is reported,[2,15] including a recent study from our group, investigating age-related gene expression differences, demonstrating higher tumor cell proliferation in the young, also when adjusting for molecular subtypes.[16]

The 50-gene PAM50 signature stratifies BC into the intrinsic subtypes luminal A, luminal B, HER2-enriched, and basal-like BCs.[17,18] Young BC patients have an increased risk for having more aggressive subtypes, and young women with early-stage BC presents with higher risk of BC recurrence.[14] In a study by Partridge et al,[14] young age was shown to be significantly associated with increased risk of BC death solely in women diagnosed with luminal A cancer. However, the relationship between risk of recurrence (ROR) within subtypes and young age at BC diagnosis and survival is not adequately addressed.

Accumulating evidence presented in recent studies indicates that the presence of tumor-infiltrating immune cells demonstrates significant associations with prognosis and response to cancer treatment.[19,20] Age-related differences in immune cell distribution have so far been little studied.[21]

The aim of this study was to explore gene expression alterations in a cohort of patients <50 years with BC, comparing the youngest (aged <40 years) with patients aged 40 to 49 years. We also wanted to examine the prognostic value of the PAM50-based molecular subtypes and risk groups in a population aged <50 years with BC and how the immune cell types (by messenger RNA [mRNA] markers) are distributed in BC of the young. We applied mRNA expression profiling by NanoString BC360 panel on archived formalin-fixed paraffin-embedded (FFPE) material from a BC cohort with long and complete follow-up. Results were validated in the Molecular Taxonomy of Breast Cancer International Consortium (METABRIC) cohort.

Materials and Methods

Patient Cohort

The study included the Bergen in-house cohort of 355 BC patients aged <50 years at time of diagnosis, residing in Hordaland County, Norway, and diagnosed with primary invasive BC during the period January 1996 and January 2003[22] (Supplemental Fig. S1). Information on the clinicopathologic variables histologic type and grade, lymph node status, tumor diameter, and hormone receptor status were obtained through the local pathology registry at Department of Pathology, Haukeland University Hospital, Bergen.

The follow-up information acquired from the Norwegian Cause of Death Registry was considered accurate and complete and included information on follow-up time, status at last follow-up, and cause of death. The last date of follow-up was June 30, 2017. Median follow-up time of survivors was 175 months (range, 13-257 months).

The study was approved by the Western Regional Committee for Medical and Health Research Ethics, REC West (2014/1984/ Regionale komiteer for medisinsk og helsefaglig forskningsetikk [REK] vest). The informed consent was waived by the REK ethics committee.

Standard Breast Cancer Immunohistochemistry Markers

For the in-house cohort, primary tumor tissue blocks were available for 339 of the cases (95.5%). The tissue was fixed following standard protocol at the time, using 4% buffered formaldehyde before processing and further paraffin embedding. The FFPE blocks were stored for up to 26 years (range, 20-26 years).

In the in-house cohort, estrogen receptor (ER) α and progesterone receptor (PR) immunohistochemical data were obtained from the routine pathology reports or by additional immunohistochemistry (IHC).[22] The cut points for ER and PR positivity were kept at 10% staining, in accordance with clinical practice at the time of diagnosis. The established scoring system for DAKO Herceptest was used.[23] HER2 Silver *In Situ* Hybridization (SISH) was performed on IHC 2+ cases (Ventana INFORM HER2 DNA probe staining). Cases were scored 0, 1+, 2+, or 3+ based on intensity grade of membrane staining and percentage of tumor cells with such staining. Cases with 0 and 1+ scores were classified as negative, and 3+ as positive. HER2 SISH was performed on IHC 2+ cases (Ventana INFORM HER2 DNA probe staining). The 2+ cases were considered HER2 positive if the HER2/Chr17 ratio by SISH was $\geq$2.0.[24,25] Ki67 was assessed by IHC on tissue microarrays (TMA) or whole sections when the case was not available in the TMA.[22] The molecular subtypes were originally classified using ER, PR, HER2, and Ki67 immunohistochemical markers, as recommended in the St Gallen guidelines 2013.[22,26]

RNA Extraction and NanoString Profiling Setup

To obtain mRNA gene expression profiles from FFPE BC tissues, we applied the NanoString BC360 panel and the nCounter platform. Among the 339 BC patients preselected for mRNA extraction, 126 patients were excluded owing to various reasons (Supplemental Fig. S1). Previous punching of tumor tissue cores for TMA from the whole cohort entailed a rather high number of excluded cases owing to scarcity of tumor tissue. RNA extraction was obtained for 213 tumor samples. Briefly, FFPE tissue mounted on hematoxylin-and-eosin–stained slides were reviewed by an experienced pathologist (E.W.), marking tumor areas for RNA extraction. Using the tumor-marked hematoxylin-and-eosin–-stained slides as templates, tumor-containing areas were macrodissected from 10-μm–sectioned unstained slides and processed for RNA isolation using the following kits (according to the manufacturer's instruction): High Pure FFPET RNA Isolation Kit (Roche Diagnostics) and E.Z.N.A. FFPE RNA Kit (Omega Bio-tek). RNA purity and quality were assessed with NanoDrop 1000 Spectrophotometer (Thermo Fisher Scientific) and 4200 TapeStation system (Agilent), applying Agilent TapeStation Analysis software

(version A.02.02) and Agilent 2100 bioanalyzer (Agilent Technologies), respectively. The RNA was considered adequate for subsequent NanoString analyses, when the following purity and quality requirements were met; optical density A260/280: 1.75-2.2, A260/230: 1.45-2.2. After quality control (QC) of the mRNA, additional 83 samples were excluded owing to highly fragmented mRNA of <200 nucleotides (distribution value 200 of <50%), and 1 patient was excluded owing to too low sample amount (<25 ng). Finally, samples from 129 patients qualified for mRNA expression analyses (Supplemental Fig. S1).

For each sample, 300 ng of RNA was hybridized to the human nCounter Breast Cancer 360 (BC360) gene expression panel and signal reads processed by the nCounter platform (NanoString Technologies) according to manufacturer's protocols.[27] In brief, the reporter probe, total RNA, and a capture probe were hybridized overnight (20 hours) at 65 °C in hybridization buffer. The BC360 panel includes relevant genes for breast tumor biology and consists of 776 individual genes, of which 18 were housekeeping (HK) control genes for normalization and 40 gene signatures. The nCounter Profiler system was used to generate multiplexed digital measurements (ie, reporter-code counts) of the relative abundance of mRNA transcripts by sequence-specific probes.

Preprocessing and Normalization of NanoString mRNA Expression Data

Preprocessing of the mRNA expression data were performed using nSolver (version 4.0, supported by dependent software R; version 3.3.2; https://cran.r-project.org). Full QC started with inspection of the raw data, assessment of HK genes, and data visualization.[28] Normalization of gene counts followed the nCounter Advanced Analysis protocol by dividing counts with the geometric mean of the housekeeper gene probes count from the same lane.[28] Normalized gene expression data were log2-transformed and applied for analyses on single gene expression data and gene signatures.

PAM50 Molecular Subtypes and Risk of Recurrence Score

The 129-sample in-house gene expression data set was analyzed using the Research Use Only (RUO) version of the NanoString PAM50 algorithm, classifying each subject into an intrinsic molecular subtype: luminal A, luminal B, basal-like, and HER2-enriched BCs. The molecular subtypes of PAM50 measures the expression level of 50 genes, 8 HK genes for signal normalization, and 6 positive and 8 negative controls.[29-33] Absolute HK geomean cutoff were 202 (samples of HK geomean <202 were regarded as fail, range 202-404 as borderline, and >404 as pass). Two of the 129 samples did not meet the QC requirements and were excluded. Three samples presented borderline QC but were included for further analysis. Thus, 127 samples were eligible for downstream analyses (Supplemental Fig. S1).

The PAM50 ROR score (range, 0-100; low = 0-40, intermediate = 41-60, and high = 61-100) was calculated by using weighted coefficients to the 4 molecular subtypes (luminal A, luminal B, HER2-enriched, and basal-like BCs), the tumor size (dichotomized into ≤2.0 cm and >2.0 cm), and a proliferation score.[17,29,31]

NanoString mRNA Gene Expression Analyses

Data were analyzed by the software ROSALIND (version 3.35.13.0; https://rosalind.onramp.bio/) and nSolver (version 4.0). Fold changes and significance scores were calculated as described in the nCounter Advanced Analysis 2.0 NanoString User Manual.[28] Significant *P* values ($P < .05$) were adjusted for multiple comparisons using the Benjamini-Hochberg method of estimating false discovery rates.[34] Differentially expressed genes (DEGs) between tumors in patients aged <40 and 40 to 49 years at the time of diagnosis were identified. Volcano plots of differential expression data were plotted using the −log10 (*P* value) and log2 fold change.

External Gene Expression Data Set

For validation of results from in-house gene expression analyses, we applied the publicly available gene expression data set from the METABRIC; discovery cohort, n = 939,[35] including global mRNA gene expression data from primary BC with clinicopathologic data and follow-up information. For valid comparison with our 127 samples in-house cohort, we set an age cutoff of <50 years and excluded the normal-like subtype, resulting in a METABRIC subcohort of 204 patient samples. Among the 204 cases, 53 (26%) were aged <40 years at diagnosis whereas 151 (74%) were at age 40 to 49 years.

Cluster Analysis

The M3C consensus clustering algorithm (Monte Carlo simulation, R v 1.20.0)[36] was used to estimate the optimal number of clusters in unsupervised clustering analysis, evaluated in our data to 4 clusters (K = 4) as optimum. Generation of heatmaps and clusters were performed with the heatmapR package.

Functional Enrichment Analysis

DEGs were explored in OncoEnrichR (Galaxy v1.0.7 https://oncotools.elixir.no/), a bioinformatics tool for exploratory analyses, querying gene sets along dimensions such as cancer aberration frequencies, protein-protein interactions, pathway enrichment, subcellular compartment localization, target druggability, gene fitness scores, and tissue/cell-type specificity.[37]

List of DEGs were analyzed with g:Profiler,[38] Functional enrichment analysis was performed by g:GOSt (https://biit.cs.ut.ee/gprofiler/gost), using default settings and selecting Kyoto Encyclopedia of Genes and Genomes,[39] Gene Ontology (Biological Processes), Reactome,[40] and WikiPathways databases.[41]

Tumor Inflammation Score

We analyzed the Tumor Inflammation Signature (TIS) score across clusters and age groups, a validated 18-gene classifier measuring a suppressed adaptive immune response predicting response to immune checkpoint blockade.[42,43] The signature provides information about a "hot" or "cold" immune status and has in previous publications been analyzed in various cancers.[44-46]

Evaluation of Immune Cell Infiltration

For evaluation of immune cell composition between age groups in the in-house and METABRIC cohorts, the gene expression data were analyzed using the Cell-type Identification by Estimating Relative Subsets of known RNA Transcripts

(CIBERSORT; https://cibersortx.stanford.edu/) algorithm).[47] The CIBERSORT gene signature containing 547 genes was used to distinguish 22 human hematopoietic cell phenotypes. The cell types inferred by CIBERSORT were naïve B cells; memory B cells; plasma cells; CD8 T cells; naïve CD4 T cells; resting memory CD4 T cells; active memory CD4 T cells; follicular helper T cells; regulatory T cells; gamma delta T cells; resting natural killer cells; active natural killer cells; monocytes; M0, M1, and M2 macrophages; resting dendritic cells; active dendritic cells; resting mast cells; active mast cells; eosinophils; and neutrophils. A CIBERSORT *P* value of <.05 was regarded significant. The number of permutations for the statistical analyses in CIBERSORT were 100.[47]

Only the 776 genes overlapping NanoString BC360 panel were analyzed in the METABRIC data set when comparing output from the CIBERSORT analysis between the in-house and METABRIC data sets. To note, we performed the CIBERSORT analysis also in the complete METABRIC cohort to confirm that our "downscaled" METABRIC cohort (776 genes, patients aged <50 years) were representative.

Statistical Methods

For statistical analyses, SPSS (version 25.0; IBM) was applied. Categories were compared using Pearson χ^2 or Fisher exact tests when appropriate. Spearman rank correlation test was applied when comparing bivariate continuous variables, and Spearman correlation coefficients (ρ) were reported. When analyzing differences in distribution of continuous variables between 2 or more categories, Mann-Whitney U or Kruskal-Wallis tests were applied. For univariate survival analyses, the Kaplan-Meier product-limit method (log-rank test) was applied. Multivariate BC-specific survival analysis was performed by Cox proportional hazards regression model, with calculations done according to the enter method. Variables were included in the Cox survival analyses after evaluating their log-minus-log plot. For multivariate analyses, only patients with information on all variables were included. Death from BC was used as end point. All statistical tests were 2-sided, and statistical significance was assessed at 5% level.

Results

Patient Cohort and Clinicopathologic Data

From the 355 patients eligible for inclusion from our Bergen in-house cohort, we obtained preprocessed and quality-controlled mRNA expression profiles of 127 cases. The mean patient age for the 127 included cases was 43 years (median, 44 years; range, 26-49 years), and 34 patients (26%) were <40 years at time of diagnosis. Supplemental Table S1 presents the clinicopathologic variables for all 355 samples in the in-house cohort, split by the samples analyzed by NanoString (n = 127) and the rest of the original in-house cohort (n = 228), demonstrating that the final 127 eligible samples that qualified for downstream analyses were representative for the population-based cohort.

Age-Related Differentially Expressed Genes Present Clusters With Clinical Relevance

To gain insight into the age-related BC disease classes and biology, we used mRNA gene expression data from the 127 patients profiled with the BC360 panel, to investigate DEGs between young (aged <40 years, n = 34) and older patients (40-49 years, n = 93). We found 49 genes differentially expressed between the age groups, 28 upregulated and 21 downregulated genes in the young (fold change ±1.5; adjusted $P \leq .05$) (Fig. 1A-B; Supplemental Table S2). Eight of the 49 genes overlapped with the PAM50 gene list (*TYMS*, *CDC6*, *ANLN*, *FGFR4*, *RRM2*, *CCNE1*, *GRB7*, and *ERBB2*).

Next, we performed unsupervised hierarchical clustering of the 49 identified DEGs. The resulting heatmap demonstrated 4 patient clusters with distinct expression profiles in relation to clinicopathologic features, PAM50 subtypes and ROR classifications (Fig. 1C; Table 1). The clustering also revealed gene clusters contributing to further interpretation of the 4 patient clusters.

Cluster 1 patients were associated with small tumor size; low histologic grade; ER and PR positivity; and HER2 negativity. Further, cluster 1 was represented by a high proportion of tumors of the luminal-like subtypes and with the highest proportion of low-risk samples (47% low-risk cases) (Fig. 1C; Table 1). One of the gene clusters showed a group of highly upregulated genes in patient cluster 1, including *HOXA9*, *CACNA1D*, *AREG*, and *NR4A1*, shown to be important in tumor cell proliferation.[48-50] Further supporting the importance of proliferation in cluster 1, we observed the MAPK signaling pathway and cell cycle regulation, as well as proliferation signaling as the most significantly enriched pathways in patient cluster 1 (Supplemental Table S3).

Patients within cluster 2 were associated with high histologic grade; ER, PR, and HER2 negativity; and the basal-like subtype. In this cluster, the genes *CDK6, CCNE1*, *TYMS*, *MYCN*, *IL2RA*, and *AURKA* were upregulated and clustered together. Collectively, their upregulation indicates higher proliferation,[51-53] association with aggressive tumor phenotypes, and reduced survival.[54-57] Patients in cluster 3 associated with large tumor size; ER and PR negativity; HER2 positivity; and the HER2-enriched subtype. Strikingly, the gene subcluster in patient cluster 3 consisted of high expression of only 3 deviant genes, *ERBB2*, *GRB7*, and *FGFR4*.

Cluster 4 presented a mix of all PAM50 subtypes, although the highest representation of the luminal B subtype (Fig. 1C; Table 1), and was associated with small tumor size, low histologic grade, ER and PR positivity, and HER2 negativity (Fig. 1C; Table 1). We did not observe any particular gene subclusters in patient cluster 4. Rather, all 49 DEGs in cluster 4 were expressed with mixed expression levels across genes.

Cluster 3 patients were associated with the highest ROR score (90% high ROR score), whereas tumors in cluster 2 and 4 presented 68% and 79% with high ROR score, respectively. Cluster 1 presented 32% of cases with high ROR score and 44% with low ROR score (Fig. 1D). When investigating the survival probabilities for the clusters, we found patient cluster 3 associated with shortest disease-specific survival, whereas patients in cluster 1 presented longest survival (Fig. 1E).

When including tumor diameter, histologic grade, lymph node status, and the cluster information in the Cox multivariate survival analysis, the clusters demonstrated independent association with shorter disease-specific survival (Fig. 1F). Further, the cluster information maintained independent association with disease-specific survival also when adjusted for the molecular subtypes by IHC (cluster 3: hazard ratio, 8.31; 95% CI, 2.64-26.16; $P < .001$; cluster 4: hazard ratio, 5.27; 95% CI, 1.70-16.34; $P = .005$), and when adding the clinicopathologic variables to the Cox model (Supplemental Table S4). The same results were not seen when adjusting for the molecular subtypes by PAM50.

For comparison, unsupervised hierarchical clustering of the 49 identified DEGs in the METABRIC discovery cohort (including only samples from patients aged <50 years, see Materials and Methods section) demonstrated a heatmap that captured a similar but

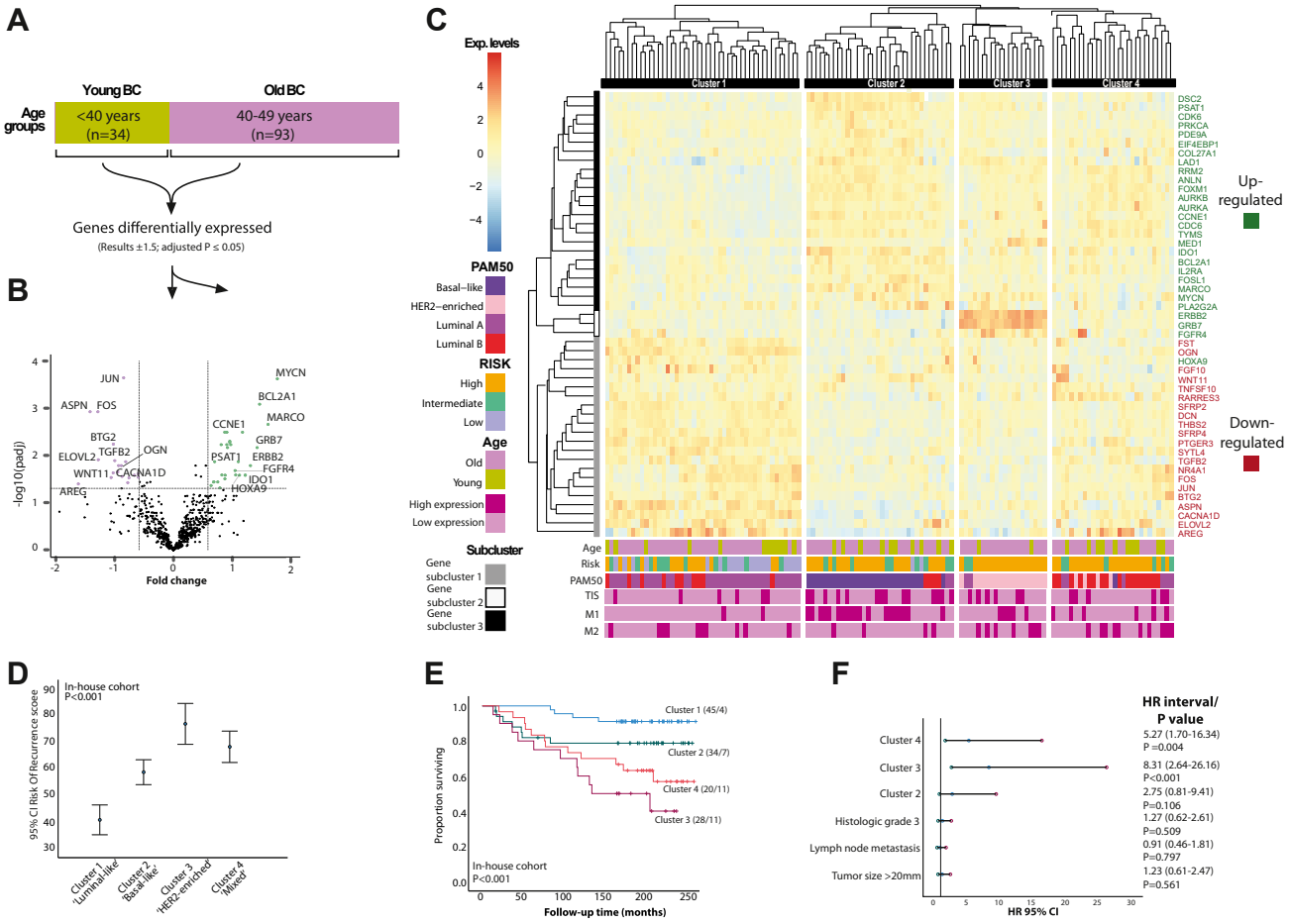

Figure 1.

Unsupervised hierarchical clustering reveals 4 patient clusters with distinct associations to risk of recurrence and survival. (A) Overview of analysis workflow, genes differentially expressed between the 2 breast cancer groups: younger than 40 years (n = 34) versus 40-49 years (n = 93). (B) Volcano plot of differentially expressed genes (DEGs) between young and older breast cancer patients. Green and purple dots represent significantly upregulated and downregulated DEGs in the young samples (aged younger than 40 years) compared with samples (aged 40-49 years; $P = .005$). (C) Unsupervised hierarchical clustering of the 49 significantly DEGs representing 4 patient clusters and 3 gene subclusters with respective PAM50 subtypes, risk of recurrence proles, TIS score, and immune profiles of M1 and M2. (D,E) Patient cluster 3 associated with the highest risk of recurrence among the 4 patient clusters (D) and the shortest disease-specific survival (E). (F) When adjusting for common prognostic variables, patient clusters 3 and 4 demonstrating independent association with shorter disease-specific survival (Cox multivariate analysis). All data from in-house cohort. Kaplan-Meier plot, numbers in brackets indicate numbers of patients/numbers of events. M1/M2, macrophages 1/2; TIS, Tumor Inflammation Signature.

stronger subtype-related cluster pattern as the one generated for the in-house cohort (Supplemental Fig. S2A). Five clusters were identified, representing 1 luminal-like (cluster 1), 2 basal-like (cluster 2 and 3), 1 HER2-enriced cluster (cluster 4), and 1 mixed cluster (cluster 5). Similar survival patterns compared with the in-house cohort were detected when performing survival analysis on these 5 clusters (Supplemental Fig. S2B).

The patient clusters from our in-house cohort were not significantly associated with the age groups (Table 1; Supplemental Fig. S3A). Of note, in the METABRIC aged <50 years cohort, we found a significantly differential distribution of clusters 1 to 4 in patients aged <40 vs 40 to 49 years, where the clusters harboring the majority of HER2-enriched and basal-like tumors were more frequently present in the youngest subgroup (Supplemental Table S5; Supplemental Fig. S3).

To further investigate the robustness of these clusters, we compared their prognostic value with our previously identified and strong prognosticator, the 6-gene proliferation score (6GPS).[16] As the NanoString BC360 panel do not completely cover the genes in the 6GPS, we instead explored the METABRIC discovery "below 50" cohort (n = 204). In this analysis, we observed significantly higher levels of the 6GPS score in the patient clusters 2 and 3 (Supplemental Fig. S3C). In cluster 1, the 6GPS presented significant prognostic value (univariate analysis) (Supplemental Fig. S3D). In the age group 40 to 49 years, the clusters presented independent prognostic value by multivariate analyses, when including the standard clinicopathologic variables tumor size, histologic grade, lymph node status, and the 6GPS score (Supplemental Table S6). In the group aged <40 years, the clusters did not maintain independent prognostic value in a similar Cox model.

Young BC Patients Associate With HER2-Enriched and Basal-Like PAM50 Subtypes, More Aggressive Clinicopathologic Characteristics, and High ROR

The NanoString RUO PAM50 algorithm was applied to determine the molecular subtypes and ROR score for the BC samples. The PAM50 gene signature provides information for each patient about the tumor intrinsic subtype (luminal A, luminal B, HER2-enriched or basal-like BCs) and the ROR score, contributing to 3

Table 1
Clinicopathologic variables across patient clusters 1-4

Variables	Patient cluster				
	Cluster 1	Cluster 2	Cluster 3	Cluster 4	*P*
	n (%)	n (%)	n (%)	n (%)	
Age (y)					NS
<40	12 (27)	10 (29)	2 (10)	10 (36)	
40-49	33 (73)	24 (71)	18 (90)	18 (64)	
Histologic grade					<.001[a]
Grade 1 or 2	41 (91)	11 (32)	11 (55)	17 (61)	
Grade 3	4 (9)	23 (68)	9 (45)	11 (39)	
Tumor size (mm)					.032[a]
≤20	31 (69)	15 (44)	8 (40)	11 (39)	
>20	14 (31)	19 (56)	12 (60)	17 (61)	
Nodal status					NS
Negative	30 (67)	17 (71)	8 (40)	15 (54)	
Positive	15 (33)	17 (29)	12 (60)	13 (46)	
ER status (IHC)					<.001[a]
Positive	42 (93)	7 (21)	7 (35)	25 (89)	
Negative	3 (7)	27 (79)	13 (65)	3 (11)	
PR status (IHC)					<.001[a]
Positive	41 (91)	8 (23)	3 (15)	20 (71)	
Negative	4 (9)	26 (77)	17 (85)	8 (29)	
HER2 status (IHC)					<.001[a]
Negative	44 (98)	33 (97)	1 (5)	27 (96)	
Positive	1 (2)	1 (3)	19 (95)	1 (4)	
Molecular subtypes (PAM50)					<.001[a]
Luminal A	35 (78)	2 (6)	2 (10)	6 (21)	
Luminal B	10 (32)	4 (12)	0	17 (61)	
HER2-enriched	0	0	18 (90)	4 (14)	
Basal-like	0	28 (82)	0	1 (4)	
Molecular subtypes (IHC)					<.001[a]
Luminal A	26 (58)	2 (5)	0	4 (14)	
Luminal B	19 (42)	7 (21)	0	23 (82)	
Luminal B HER2+	0	0	8 (40)	0	
HER2+ nonluminal	0	0	11 (55)	1 (4)	
Triple negative	0	25 (74)	1 (5)	0	
Risk group (ROR)					<.001[a]
Low	21 (47)	2 (6)	0	0	
Intermediate	10 (22)	9 (26)	2 (10)	6 (21)	
High	14 (31)	23 (68)	18 (90)	22 (79)	

Percent calculated by columns.
ER, estrogen receptor; IHC, immunohistochemistry; NS, not significant; PR, progesterone receptor; ROR, risk of recurrence.
[a] Significant differences of the variables across patient clusters are indicated by *P* value.

risk groups indicating low, intermediate, or high risk of recurrence (see Materials and Methods section). The molecular subtypes were also determined by surrogate immunohistochemical markers. When comparing the subtypes described by the PAM50 RUO algorithm and immunohistochemical markers, we found a 67% concordance between the 2 approaches, the majority of the discordance being within the luminal types (Supplemental Table S7; Supplemental Fig. S4A).

Among the PAM50-determined subtypes, the HER2-enriched and basal-like subtypes associated as expected with high histologic grade, ER and PR negative status, and the HER2 and triple-negative subtypes (determined by immunohistochemical markers), respectively (Supplemental Table S7). In the patient group <40 years, we observed 20% (n = 7) luminal A, 20% (n = 7) luminal B, 25% (n = 8) HER2-enriched, and 35% (n = 12) basal-like cases. Patients aged 40 to 49 years presented 40% (n = 38) luminal A subtype, 25% (n = 24) luminal B, 15% (n = 14) HER2-enriched, and 18% (n = 17) basal-like subtype (Supplemental Table S8).

By univariate survival analyses of PAM50 molecular subtypes, we demonstrated the shortest disease-specific survival among patients with HER2-enriched tumors (5-year and 20-year survival, 77.3% and 41.7%, respectively) (Fig. 2A), also when stratifying for age groups younger than 40 years; (5-year and 20-year survival, both 50%) and 40 to 49 years (5-year and 20-year survival, 73.7% and 48.2%, respectively) (Fig. 2B-C). To note, in this cohort of BC patients aged <50 years, the basal-like tumors associated with better survival than the luminal B subtype (5-year survival: 85.8% vs 83.9%; 20-year survival: 78.5% vs 67.2%) (Fig. 2A), also when split by the age groups <40 and 40 to 49 years (5-year and 20-year survival: 77.8% vs 64.8% in the young; 5-year survival: 79.2% vs 77.3%; 20-year survival: 79.2% versus 68.2% in the older) (Fig. 2B-C).

The IHC-based molecular subtypes associated with a similar survival pattern as the PAM50-based subtypes, where patients with luminal A and luminal B/HER2 negative subtypes presented longest survival and those with the HER2 subtype and luminal B/HER2 positive subtype associated with shortest survival (Fig. 2D). Similar as for the PAM50-based basal-like subtype, the IHC-determined triple-negative subtype associated with intermediate long survival (5-year and 20-year survival: 84.1% and 72.1%, respectively) (Fig. 2D).

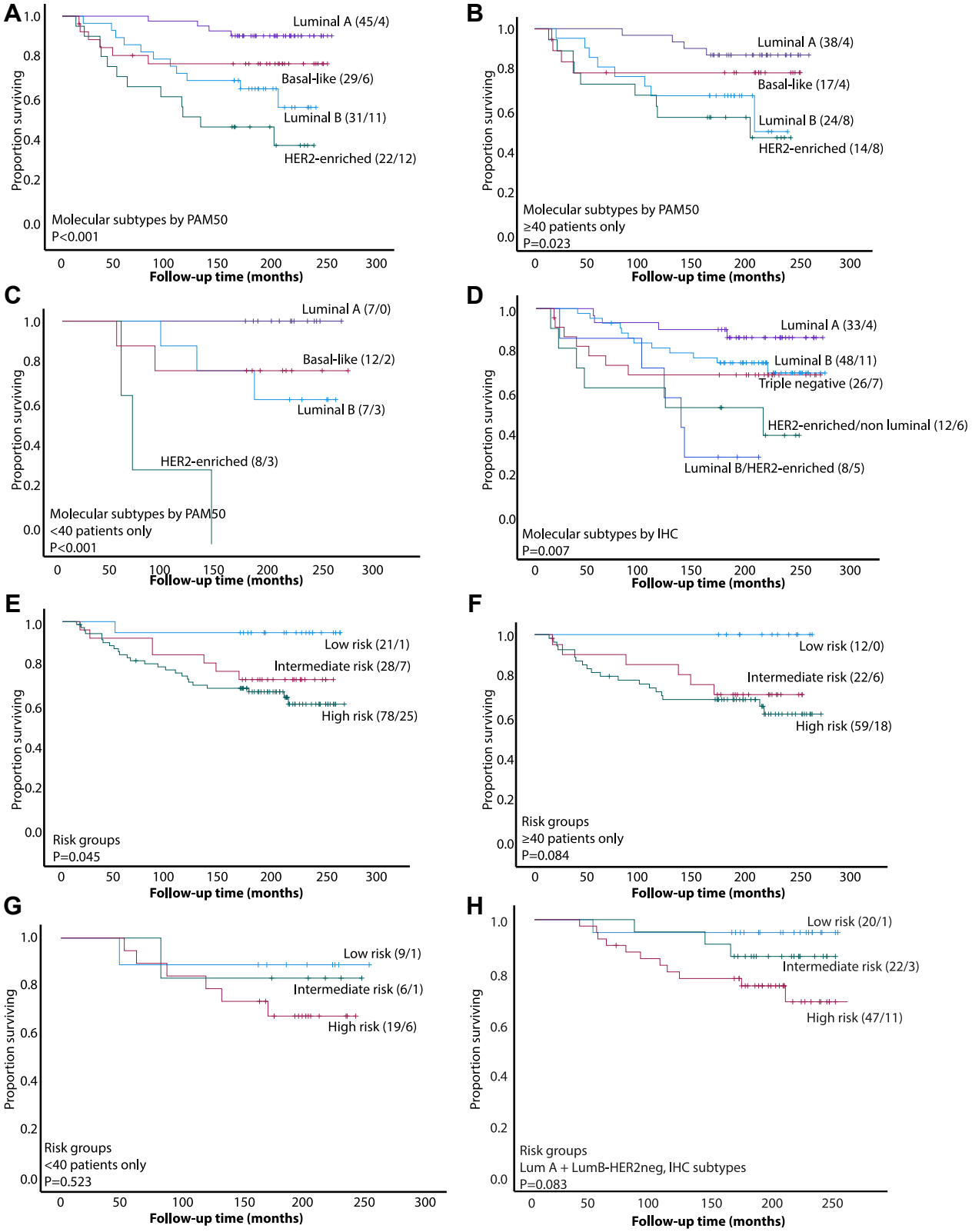

Figure 2.

Disease-specific survival according to molecular subtype, age groups, and risk of recurrence score. (A-C) HER2-enriched subtype associated with shorter disease-specific survival related to PAM50 subtypes (A, n = 127), also stratified by age groups (B, n = 93; C, n = 34). (D) Luminal B/HER2-enriched subtype associated with shorter disease-specific survival in the molecular subtypes defined by IHC (n = 127). (E-G) A high risk of recurrence score associated with shorter disease-specific survival, with a trend of significance within patients older than 40 years only (F, n = 93) but not in patients younger than 40 years (G, n = 34). (H) A trend of significance was also observed in luminal, HER2 negative patients (molecular subtypes by IHC, n = 89). All data from the in-house cohort. Kaplan–Meier plots, numbers in brackets indicate numbers of patients/numbers of events. IHC, immunohistochemistry.

Table 2
Associations between recurrence risk groups and clinicopathologic variables

Variables	Recurrence risk groups			*P*
	Low	Intermediate	High	
	n (%)	n (%)	n (%)	
Age (y)				NS
<40	9 (26)	6 (18)	19 (56)	
40-49	12 (13)	22 (23)	59 (62)	
Tumor size (mm)				.007
≤20	17 (81)	15 (54)	33 (42)	
>20	4 (19)	13 (46)	45 (58)	
Histologic grade				<.001
Grade 1 or 2	18 (86)	24 (86)	38 (49)	
Grade 3	3 (14)	4 (14)	40 (51)	
Nodal status				.006
Negative	19 (90)	20 (71)	31 (40)	
Positive	2 (5)	8 (29)	47 (60)	
ER status (IHC)				.022
Positive	18 (86)	20 (71)	43 (55)	
Negative	3 (14)	8 (29)	35 (45)	
PR status (IHC)				.015
Positive	17 (81)	18 (64)	37 (47)	
Negative	4 (19)	10 (36)	41 (53)	
HER2 (IHC)				.006
Negative	21 (100)	26 (93)	58 (74)	
Positive	0	2 (7)	20 (26)	
Molecular subtypes by (PAM50)				<.001
Luminal A	19 (90)	18 (65)	8 (10)	
Luminal B	0	4 (14)	27 (35)	
HER2-enriched	0	0	22 (28)	
Basal-like	2 (10)	6 (21)	21 (27)	
Molecular subtypes (IHC)				<.001
Luminal A	13 (62)	8 (29)	12 (15)	
Luminal B	7 (33)	13 (47)	28 (36)	
Luminal B HER2$^+$	0	1 (3)	7 (9)	
HER2$^+$ nonluminal	0	1 (3)	11 (14)	
Triple negative	1 (5)	5 (18)	20 (26)	

IHC, immunohistochemistry; NS, not significant ROR, risk of recurrence.

The PAM50-derived ROR score and information on tumor size and lymph node status provided the basis for the risk groups indicating low, intermediate, and high risk of recurrence. The high-risk group associated with large tumor size, high histologic grade, lymph node metastases, PR negative status, and HER2 negativity (Table 2).

In patients aged younger than 40 years at diagnosis, 56% (n = 19) were in the high-risk group, 18% (n = 6) in the intermediate-risk group, and 26% (n = 9) in the low-risk group. Among patients aged 40-49 years, 62% (n = 59) were in the high-risk group, 23% (n = 22) in the intermediate-risk group, and 13% (n = 12) in the low-risk group (Supplemental Table S7).

The risk groups associated with deteriorating survival from the low-risk group, presenting longest survival (5-year and 20-year survival: both 95.2%); through the intermediate-risk group (5-year and 20-year survival: 92.9% and 75.0%, respectively), to the high-risk group (5-year and 20-year survival: 84.4% and 64.4%, respectively) (Fig. 2E). A similar survival pattern was observed among patients aged 40 to 49 years only; the low-risk group presenting longest survival (no deaths from BC); through intermediate-risk group (5-year and 20-year survival: 90.9% and 72.7%, respectively), to the high-risk group (5-year and 20-year survival: 81.1% and 63.9%, respectively) (Fig. 2F). Patients aged <40 years presented a similar survival pattern as observed in patients aged 40 to 49 years, however not significant (Fig. 2G).

Moreover, among the hormone receptor positivity, HER2-negative patients, the ROR classification separated patients with different BC-specific survival—the high ROR group demonstrated shortest survival (5-year survival, 90%; 20-year survival, 68%) (Fig. 2H).

Immune Cell Distribution in Young Breast Cancer

Given the unexpected observation of better survival in patients with basal-like and triple-negative tumors compared with patients with luminal B tumors, we next sought to investigate the immune cell distribution across patient clusters and molecular subtypes, hypothesizing that immune cell differences could explain the differences in patient survival.

The tumor immune microenvironment (TIME) is known to impact cancer progress.[58,59] However, knowledge is needed to understand how age relates to TIME alterations. Deconvolution-based methods can be applied for in silico quantification of immune cell types in mRNA gene expression data from heterogeneous tumor samples.[47] We therefore examined, using in silico analyses, how the immune cell composition was distributed across patient and tumors subsets, using CIBERSORT to deconvolute the in-house and METABRIC mRNA gene expression data to reflect 22 immune cell-type populations of the tumor microenvironment in patient clusters 1-4 (Fig. 3A).

Patient cluster 1 associated with levels of expression profiles reflecting lower B memory cell counts, lower levels of M1 macrophages ($P < .002$) and CD8$^+$ T cells ($P = .05$) and showed a tendency of higher levels of neutrophil granulocytes ($P = .1$) and T helper cells ($P = .06$). Interestingly, patient cluster 2, including a large proportion of basal-like tumors, presented expression profiles reflecting higher levels of M0 and M1 macrophages ($P \leq .007$) and lower levels of M2 macrophages ($P = .001$) compared with cases in cluster 1, 3, and 4. Patient cluster 3 presented intermediate high levels of M1 macrophages and high levels of M2 macrophages ($P \leq .001$). Patient cluster 4, harboring mixed molecular subtypes, presented intermediate high levels of M1 macrophages, high levels of M2 macrophages ($P \leq .001$), and highest levels of CD4$^+$ T cells ($P = .004$).

Having identified differences in the immune cell distribution among the clusters, we hypothesized that the patient clusters and age groups present with different immune evasive properties. We therefore investigated how a TIS score, predicting response to immunotherapies in cancer,[42,43] was distributed across the clusters and age groups. We demonstrated the highest TIS score in patient cluster 2, intermediate score levels in cluster 3 and 4, and the lowest score in cluster 1 (in-house cohort) (Fig. 3B). In our in-house cohort, the TIS score was not significantly different between age groups. However, in the METABRIC cohort, we observed significantly higher levels of the TIS score in the young compared with older patients ($P = .044$) (Supplemental Fig. S4B, C).

When investigating the reflection of macrophage levels across the age groups, we did not detect significant differences. However, when examining macrophage levels across PAM50 and immunohistochemical subtypes, we observed higher levels of M2 macrophages in the HER2-enriched subtypes, compared with the basal-like and triple-negative subtypes. Further, in the basal and triple-negative subtypes, we observed higher expression of M1 macrophages, complementing the higher level of M0 and M1 macrophages detected in the basal-like enriched cluster 2 (Fig. 4A-D).

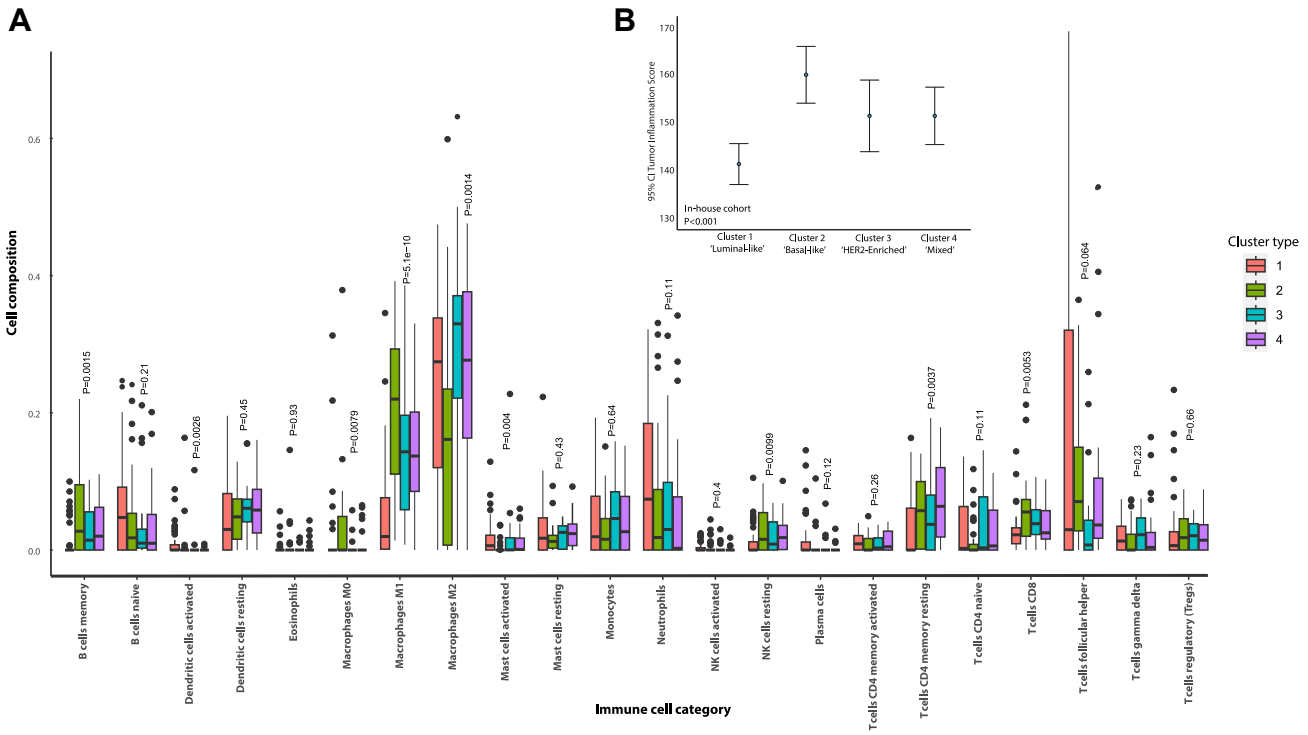

Figure 3.
Immune cell-type composition and Tumor Inflammation Signature score across patient clusters 1-4. (A) Comparison of tumor immune infiltrating cell types in the tumor microenvironment across patient clusters 1-4 from the in-house cohort. (B) Tumor Inflammation Signature score across patient cluster 1-4. Data from the in-house cohort shown with error bars representing 95% CI of the mean and *P* values by Mann–Whitney *U* test.

Discussion

Our understanding of how the BC biology and tumor microenvironment contribute to the increased tumor aggressiveness observed in young BC is inadequate. In this study, we aimed to achieve a better understanding of age-related gene expression differences in BC.

To our knowledge, this is the first study using archived FFPE material to elucidate gene expression alterations when searching for biologically relevant differences in BC of the young, in a population-based cohort with long and complete follow-up data. We have validated parts of our findings in the publicly available METABRIC (discovery) BC cohort. Moreover, to our knowledge, this is the first study investigating the validity of PAM50 and ROR specifically in a young, population-related BC cohort.

Based on empirical data from a previous study by our group[22] and European School of Oncology and European Society of Medical Oncology (ESO-ESMO) guidelines (from International Consensus Conferences for Breast Cancer in Young Women[60-65]), we defined "young BC" as patients aged <40 years at diagnosis. We identified age-based patient clusters with distinct clinicopathologic features, TIS score, and macrophage subtype profiles. When including the classic clinicopathologic variables and the cluster information in a Cox multivariate survival analysis, the clusters demonstrated independent association with shorter disease-specific survival, also when adjusting for the IHC-based molecular subtypes. When including our previously derived 6GPS,[16] the clusters maintained independent prognostic value in the age group 40 to 49 years, supporting their prognostic value, and the added value of applying cluster-based analysis approaches as supplementary to signature analyses.

Our results indicated better survival than expected in patients with triple-negative (IHC-based) and basal-like (PMA50-based) subtypes in the cohort of patients aged <50 years.[66] The same trend was observed within the detected patient clusters, where the basal-like enriched cluster 2 demonstrated better survival than the clusters reflecting the HER2-enriched subtype and mixed subtypes. These findings are in line with other studies investigating survival according to the molecular subtypes; the HER2 subtype has been associated with poorer survival, compared with the basal-like subtype.[66,67]

PAM50 intrinsic subtyping and ROR score are approved for risk profiling in postmenopausal women with ER-positive, HER2-negative tumors.[68-70] In premenopausal women, the prognostic value of PAM50 subtypes and the ROR score is still not clear, but studies have indicated that PAM50 and the ROR score are applicable in this patient group.[66,71,72]

In line with previous studies on the ROR score in populations with mixed ages, usually including none or only a few young BC patients,[66,70,72] we demonstrated deteriorating survival from the low-risk, intermediate-risk, to the high-risk groups in patients aged 40 to 49 years and a similar trend in younger patients aged <40 years. Also, among patients with hormone receptor–positive, HER2-negative tumors, the risk of recurrence classifier separated patients with different BC-specific survival, with the shortest survival assigned to the group determined to be of high ROR. This is in line with a previous study showing that among patients with HR-positive, HER2-negative tumors, the ROR classification separated patients with distinct BC-specific survival.[66] Our results support the prognostic validity of the clinical application of ROR also in a young BC cohort.

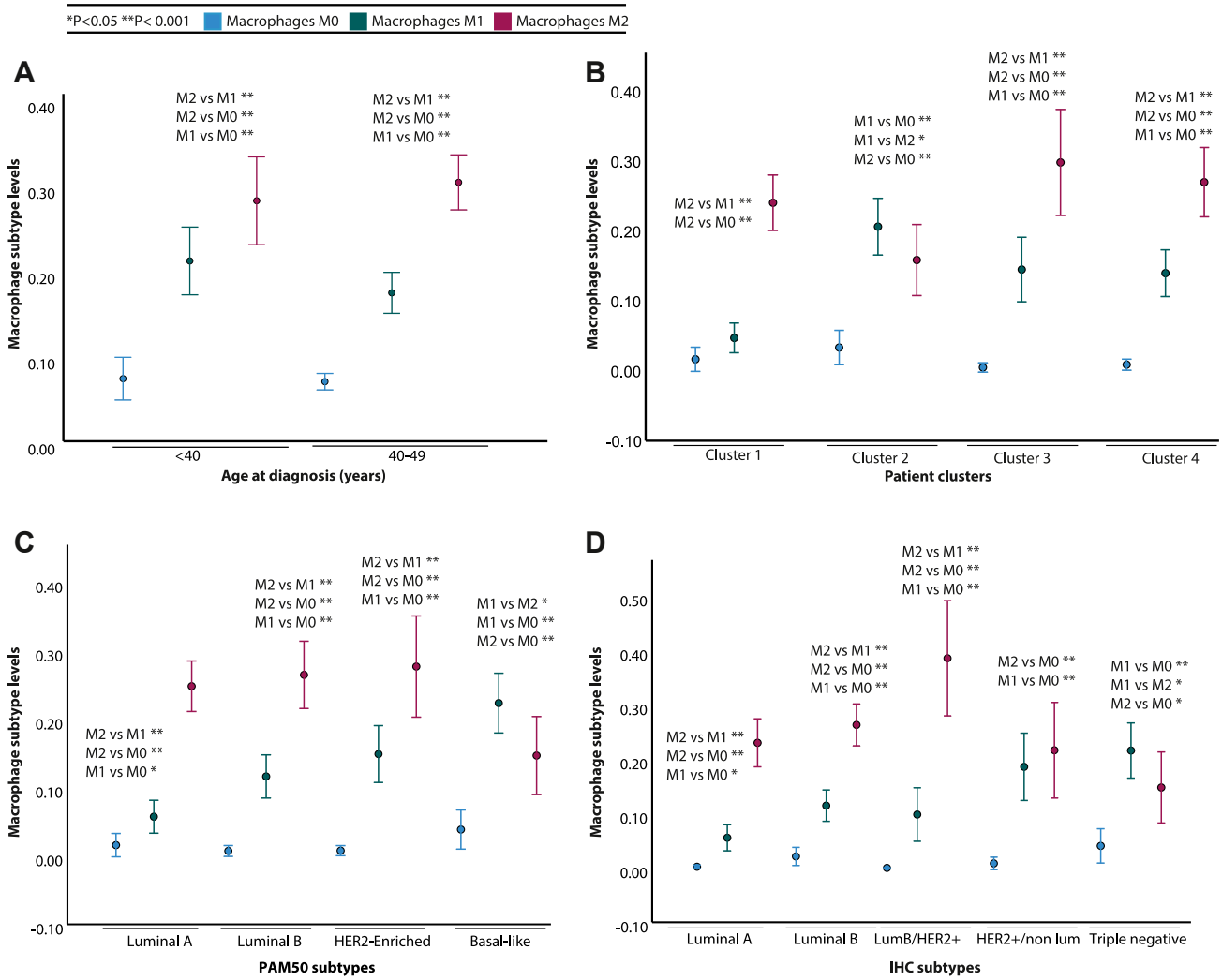

Figure 4.

Macrophage subtype levels across age groups, patient clusters and molecular subtypes determined by PAM50 and IHC. (A-D) Expression of M0, M1, and M2 macrophages across age at diagnosis (A), patient cluster 1-4 (B), PAM50 subtypes (C), and immunohistochemical subtypes (D). All data obtained from in-house NanoString expression cohort (n = 127). Levels of significance (*$P = .05$) and high significance (**$P = .001$) indicated. IHC, immunohistochemistry.

It should be noted that our retrospective in-house cohort were obtained at a time before the introduction of anti-HER2 therapies and immunotherapy options in Norway, leaving chemotherapy and radiation as the adjuvant treatment options. The <50 years group of BC patients is outside the breast screening program in Norway, allowing studies on the natural BC course, not affected by the detection mode (screening/interval). This provides relevance for applying the 49 to 49 years group as comparator when studying BC in the <40 years group.

The immune components of the tumor have gained increasing focus over the past years. M0 and M1 macrophages are associated with antitumor activities[19] and M2 macrophages with protumor (immune-inhibitory) activities.[73,74] We observed higher levels of M0 and M1 macrophages than those of M2 macrophages in patient cluster 2 and the triple-negative and basal-like subtypes, which might suggest a rationale for the survival prospects that were better than anticipated for these patients, despite the lack of immunotherapies and other targeted treatments at the time being.

A recent study discovered that tumors in young BC patients present higher expression of immune-related genes compared with those in older women, which implies a more active antitumor immune response,[75] supporting our results of higher M0 and M1 macrophages in the triple-negative and basal-like subtypes. The general aging process is associated with declining immune function, immunosenescence, but studies focusing on age-related differences in the breast TIME are lacking.[76,77] Young BC patients are suggested to gain improved response to immunotherapy owing to on an immune-activated TIME compared with older BC patients.[78] A high TIS score has previously been associated with improved response to PD-1 inhibitory therapies and prolonged survival across cancer types.[45] In this study, we demonstrated an elevated TIS score in the young cohort, potentially resulting in altered immune responses and supporting anticipated improved response to immunotherapies. Age-related distribution of immune cells in BC is still an unexplored field. Future well-designed studies are imperative to further validate our findings.

In this study, we experienced a higher failure/exclusion rate of cases for NanoString BC360 analyses than would have been expected based on experiences from use of Prosigna in the clinical setting. We studied tumor tissue from archived FFPE material from the period 1996-2003. Although difficult to verify, a change

in surgical procedures, tissue fixation, and other preanalytical factors over these years may have influenced the RNA quality in our material. Previous studies have shown an impact on RNA quality from prolonged time between tissue dissection and fixation, as well as prolonged tissue fixation, and other preanalytical factors.[79,80]

Today, the smaller (targeted) surgical resections are more commonly performed than mastectomies, and the larger breast resections are sectioned early after surgery, to provide more proper formalin fixation to all parts of the specimen. We speculate whether lack of pregross sectioning of mastectomy specimens in the early periods of the study period may have provided risk of poorer RNA quality when compared with the samples assessed by PAM50/Prosigna today.

The relatively low number of genes (n = 776) in the BC360 panel provides limited information compared with global assays such as microarray or RNA sequencing approaches. Moreover, we lack information on menopausal status and *BRCA1/2* mutations, considered carrying valuable information when discussing age-related prognostic markers in BC. Further, BC patients aged <40 years are still a poorly represented group in public data sets, limiting the statistical power for subgroup analyses. In this study, a low number of patients aged <40 years provide a risk of low sensitivity to detect true differences between groups. The analyses on the in-house cohort should be considered exploratory and needs to be validated, as done for parts of the results in the larger independent METABRIC cohort, reflecting validity of the results from the in-house cohort.

In conclusion, we identify age-based patient clusters with distinct clinicopathologic features, associations with molecular subtypes, and ROR. Further, our results indicate higher levels of M0 and M1 macrophages in the triple-negative and basal-like subtypes, potentially contributing to the better survival seen in these patient subsets. Moreover, our study supports the applicability of ROR as a prognostic valid classification algorithm in young BC patients. Our results demonstrate new biomarkers that potentially may add information to the established tools for diagnosis and prognostication in BC of the young.

Acknowledgments

The authors thank Ingeborg Winge, Randi Hope Lavik, and Bendik Nordanger for their excellent technical assistance.

Author Contributions

E.W. conceived and designed the study and contributed to pathology review of tumor sections, data analysis and interpretation, and writing of the manuscript. L.M.I., L.A.A., and E.A.H. contributed to the study design, data analyses and interpretation, and writing the manuscript. A.A.S. performed the tissue-based work and immunohistochemistry, statistical analysis, and data interpretation. G.K. participated in data collection and interpretation and training in Ki67 assessment. L.M.I., A.K.M.S., R.O.C.H., K.T., M.B.K., T.A., A.H., C.A., I.M.S., L.A.A., E.A.H., and E.W. participated in data collection and interpretation. L.M.I., L.A.A., E.A.H., and E.W. wrote the manuscript with critical input from all coauthors. All authors read and approved the final manuscript.

Data Availability

Public gene expression datasets (METABRIC) are available at https://ega-archive.org/studies/EGAS00000000083. Restrictions apply to data generated within this study—these are therefore not publicly available. However, on reasonable request, interested researchers may contact corresponding author to inquire about access. Request for noncommercial use will be considered and will require full ethics review.

Funding

The research was supported by grants from the University of Bergen, Helse Vest research fund (F-12143), and the Research Council of Norway through its Centres of Excellence funding scheme (project number 223250) The results are in part based on data generated by the METABRIC consortium. The funding sources were not involved in the study other than financial support.

Declaration of Competing Interest

None reported.

Ethics Approval and Consent to Participate

The study was approved by the Western Regional Committee for Medical and Health Research Ethics, REC West (2014/1984/REK vest). Written informed consent was waived by the ethics committee. The national identification numbers of all patients were checked with the Registry of Withdrawal from Biological Research Consent by the Norwegian Institute of Public Health. None of the cases were listed in the registry.

Supplementary Material

The online version contains supplementary material available at https://doi.org/10.1016/j.modpat.2024.100529.

References

1. Sung H, Ferlay J, Siegel RL, et al. Global Cancer Statistics 2020: GLOBOCAN estimates of incidence and mortality worldwide for 36 cancers in 185 countries. *CA Cancer J Clin*. 2021;71(3):209–249.
2. Anders CK, Hsu DS, Broadwater G, et al. Young age at diagnosis correlates with worse prognosis and defines a subset of breast cancers with shared patterns of gene expression. *J Clin Oncol*. 2008;26(20):3324–3330.
3. Azim Jr HA, Partridge AH. Biology of breast cancer in young women. *Breast Cancer Res*. 2014;16(4):427.
4. Fabiano V, Mandó P, Rizzo M, et al. Breast cancer in young women presents with more aggressive pathologic characteristics: retrospective analysis from an Argentine National Database. *JCO Glob Oncol*. 2020;6:639–646.
5. Abdel-Razeq H, Iweir S, Abdel-Razeq R, et al. Differences in clinicopathological characteristics, treatment, and survival outcomes between older and younger breast cancer patients. *Sci Rep*. 2021;11(1):14340.
6. Yazdani-Charati R, Hajian-Tilaki K, Sharbatdaran M. Comparison of pathologic characteristics of breast cancer in younger and older women. *Caspian J Intern Med*. 2019;10(1):42–47.
7. Freedman RA, Partridge AH. Emerging data and current challenges for young, old, obese, or male patients with breast cancer. *Clin Cancer Res*. 2017;23(11):2647–2654.
8. Johnson RH, Chien FL, Bleyer A. Incidence of breast cancer with distant involvement among women in the United States, 1976 to 2009. *JAMA*. 2013;309(8):800–805.
9. Leclère B, Molinié F, Trétarre B, Stracci F, Daubisse-Marliac L, Colonna M. Trends in incidence of breast cancer among women under 40 in seven European countries: a GRELL cooperative study. *Cancer Epidemiol*. 2013;37(5):544–549.
10. Nguyen DV, Kim SW, Oh YT, et al. Local recurrence in young women with breast cancer: breast conserving therapy vs. mastectomy alone. *Cancers (Basel)*. 2021;13(9):2150.
11. Ademuyiwa FO, Cyr A, Ivanovich J, Thomas MA. Managing breast cancer in younger women: challenges and solutions. *Breast Cancer: Targets and Therapy*. 2016;8:1–12.
12. Waks AG, Kim D, Jain E, et al. Somatic and germline genomic alterations in very young women with breast cancer. *Clin Cancer Res*. 2022;28(11):2339–2348.

13. Gómez-Flores-Ramos L, Castro-Sánchez A, Peña-Curiel O, Mohar-Betancourt A. Molecular biology in young women with breast cancer: from tumor gene expression to DNA mutations. *Rev Invest Clin*. 2017;69(4):181–192.
14. Partridge AH, Hughes ME, Warner ET, et al. Subtype-dependent relationship between young age at diagnosis and breast cancer survival. *J Clin Oncol*. 2016;34(27):3308–3314.
15. Fredholm H, Magnusson K, Lindström LS, et al. Breast cancer in young women and prognosis: how important are proliferation markers? *Eur J Cancer*. 2017;84:278–289.
16. Ingebriktsen LM, Finne K, Akslen LA, Wik E. A novel age-related gene expression signature associates with proliferation and disease progression in breast cancer. *Br J Cancer*. 2022;127(10):1865–1875.
17. Nielsen TO, Parker JS, Leung S, et al. A comparison of PAM50 intrinsic subtyping with immunohistochemistry and clinical prognostic factors in tamoxifen-treated estrogen receptor-positive breast cancer. *Clin Cancer Res*. 2010;16(21):5222–5232.
18. Perou CM, Sørlie T, Eisen MB, et al. Molecular portraits of human breast tumours. *Nature*. 2000;406(6797):747–752.
19. Pruneri G, Vingiani A, Denkert C. Tumor infiltrating lymphocytes in early breast cancer. *Breast*. 2018;37:207–214.
20. Ziai J, Gilbert HN, Foreman O, et al. CD8+ T cell infiltration in breast and colon cancer: a histologic and statistical analysis. *PLoS One*. 2018;13(1), e0190158.
21. Jin YW, Hu P. Tumor-infiltrating CD8 T cells predict clinical breast cancer outcomes in young women. *Cancers (Basel)*. 2020;12(5):1076.
22. Svanøe AA, Humlevik ROC, Knutsvik G, et al. Age-related phenotypes in breast cancer: a population-based study. *Int J Cancer*. 2024;154(11):2014–2024.
23. Wolff AC, Hammond MEH, Allison KH, et al. Human epidermal growth factor receptor 2 testing in breast cancer: American Society of Clinical Oncology/College of American Pathologists Clinical Practice Guideline Focused Update. *J Clin Oncol*. 2018;36(20):2105–2122.
24. Rhodes A, Jasani B, Anderson E, Dodson AR, Balaton AJ. Evaluation of HER-2/neu immunohistochemical assay sensitivity and scoring on formalin-fixed and paraffin-processed cell lines and breast tumors: a comparative study involving results from laboratories in 21 countries. *Am J Clin Pathol*. 2002;118(3):408–417.
25. Knutsvik G, Stefansson IM, Aziz S, et al. Evaluation of Ki67 expression across distinct categories of breast cancer specimens: a population-based study of matched surgical specimens, core needle biopsies and tissue microarrays. *PLoS One*. 2014;9(11), e112121.
26. Goldhirsch A, Winer EP, Coates AS, et al. Personalizing the treatment of women with early breast cancer: highlights of the St Gallen International Expert Consensus on the Primary Therapy of Early Breast Cancer 2013. *Ann Oncol*. 2013;24(9):2206–2223.
27. NanoString Technologies. nCounter® Breast Cancer 360™ Panel 2021. Accessed April 28, 2021. https://www.nanostring.com/products/ncounter-assays-panels/oncology/breast-cancer-360/
28. User Manual. NanoString Technologies®. nCounter Advanced Analysis 2.0 Plugin for nSolver Software; NanoString. 2018.
29. Wallden B, Storhoff J, Nielsen T, et al. Development and verification of the PAM50-based Prosigna breast cancer gene signature assay. *BMC Med Genomics*. 2015;8:54.
30. Sestak I, Cuzick J, Dowsett M, et al. Prediction of late distant recurrence after 5 years of endocrine treatment: a combined analysis of patients from the Austrian breast and colorectal cancer study group 8 and arimidex, tamoxifen alone or in combination randomized trials using the PAM50 risk of recurrence score. *J Clin Oncol*. 2015;33(8):916–922.
31. Parker JS, Mullins M, Cheang MC, et al. Supervised risk predictor of breast cancer based on intrinsic subtypes. *J Clin Oncol*. 2009;27(8):1160–1167.
32. Geiss GK, Bumgarner RE, Birditt B, et al. Direct multiplexed measurement of gene expression with color-coded probe pairs. *Nat Biotechnol*. 2008;26(3):317–325.
33. Nielsen T, Wallden B, Schaper C, et al. Analytical validation of the PAM50-based Prosigna Breast Cancer Prognostic Gene Signature Assay and nCounter Analysis System using formalin-fixed paraffin-embedded breast tumor specimens. *BMC Cancer*. 2014;14:177.
34. Ferreira JA. The Benjamini-Hochberg method in the case of discrete test statistics. *Int J Biostat*. 2007;3(1). Article 11.
35. Curtis C, Shah SP, Chin SF, et al. The genomic and transcriptomic architecture of 2,000 breast tumours reveals novel subgroups. *Nature*. 2012;486(7403):346–352.
36. John CR, Watson D, Russ D, et al. M3C: Monte Carlo reference-based consensus clustering. *Sci Rep*. 2020;10(1):1816.
37. Nakken S, Gundersen S, Bernal FLM, Polychronopoulos D, Hovig E, Wesche J. OncoEnrichR: cancer-dedicated gene set interpretation. *arXiv preprint*. 2021. *arXiv*:2107.13247.
38. Raudvere U, Kolberg L, Kuzmin I, et al. g:Profiler: a web server for functional enrichment analysis and conversions of gene lists (2019 update). *Nucleic Acids Res*. 2019;47(W1):W191–W198.
39. Kanehisa M, Sato Y, Furumichi M, Morishima K, Tanabe M. New approach for understanding genome variations in KEGG. *Nucleic Acids Res*. 2019;47(D1):D590–D595.
40. Fabregat A, Jupe S, Matthews L, et al. The reactome pathway knowledgebase. *Nucleic Acids Res*. 2018;46(D1):D649–D655.
41. Slenter DN, Kutmon M, Hanspers K, et al. WikiPathways: a multifaceted pathway database bridging metabolomics to other omics research. *Nucleic Acids Res*. 2018;46(D1):D661–D667.
42. Ayers M, Lunceford J, Nebozhyn M, et al. IFN-γ-related mRNA profile predicts clinical response to PD-1 blockade. *J Clin Invest*. 2017;127(8):2930–2940.
43. NanoString Technologies® I. nCounter® Breast Cancer 360™ Panel 2023. Accessed June 11, 2024. https://nanostring.com/products/ncounter-assays-panels/oncology/breast-cancer-360/
44. Danaher P, Warren S, Lu R, et al. Pan-cancer adaptive immune resistance as defined by the Tumor Inflammation Signature (TIS): results from The Cancer Genome Atlas (TCGA). *J Immunother Cancer*. 2018;6(1):63.
45. Damotte D, Warren S, Arrondeau J, et al. The tumor inflammation signature (TIS) is associated with anti-PD-1 treatment benefit in the CERTIM pan-cancer cohort. *J Transl Med*. 2019;17(1):357.
46. Millar E, Browne L, Slapetova I, et al. TILs immunophenotype in breast cancer predicts local failure and overall survival: analysis in a large radiotherapy trial with long-term follow-up. *Cancers (Basel)*. 2020;12(9):2365.
47. Newman AM, Steen CB, Liu CL, et al. Determining cell type abundance and expression from bulk tissues with digital cytometry. *Nat Biotechnol*. 2019;37(7):773–782.
48. Catterall WA. Voltage-gated calcium channels. *Cold Spring Harb Perspect Biol*. 2011;3(8):a003947.
49. Phan NN, Wang CY, Chen CF, Sun Z, Lai MD, Lin YC. Voltage-gated calcium channels: novel targets for cancer therapy. *Oncol Lett*. 2017;14(2):2059–2074.
50. Schmucker H, Blanding WM, Mook JM, et al. Amphiregulin regulates proliferation and migration of HER2-positive breast cancer cells. *Cell Oncol (Dordr)*. 2018;41(2):159–168.
51. Diril MK, Ratnacaram CK, Padmakumar VC, et al. Cyclin-dependent kinase 1 (Cdk1) is essential for cell division and suppression of DNA re-replication but not for liver regeneration. *Proc Natl Acad Sci U S A*. 2012;109(10):3826–3831.
52. Du R, Huang C, Liu K, Li X, Dong Z. Targeting AURKA in cancer: molecular mechanisms and opportunities for cancer therapy. *Mol Cancer*. 2021;20(1):15.
53. Zhao ZM, Yost SE, Hutchinson KE, et al. CCNE1 amplification is associated with poor prognosis in patients with triple negative breast cancer. *BMC Cancer*. 2019;19(1):96.
54. Ways DK, Kukoly CA, deVente J, et al. MCF-7 breast cancer cells transfected with protein kinase C-alpha exhibit altered expression of other protein kinase C isoforms and display a more aggressive neoplastic phenotype. *J Clin Invest*. 1995;95(4):1906–1915.
55. Schafer JM, Lehmann BD, Gonzalez-Ericsson PI, et al. Targeting MYCN-expressing triple-negative breast cancer with BET and MEK inhibitors. *Sci Transl Med*. 2020;12(534):eaaw8275.
56. He L, Zhang W, Yang S, et al. Impact of genetic variants in IL-2RA and IL-2RB on breast cancer risk in Chinese Han women. *Biochem Genet*. 2021;59(3):697–713.
57. Song S, Tian B, Zhang M, et al. Diagnostic and prognostic value of thymidylate synthase expression in breast cancer. *Clin Exp Pharmacol Physiol*. 2021;48(2):279–287.
58. Chew V, Toh HC, Abastado JP. Immune microenvironment in tumor progression: characteristics and challenges for therapy. *J Oncol*. 2012;2012, 608406.
59. Binnewies M, Roberts EW, Kersten K, et al. Understanding the tumor immune microenvironment (TIME) for effective therapy. *Nat Med*. 2018;24(5):541–550.
60. Cardoso F, Kyriakides S, Ohno S, et al. Early breast cancer: ESMO Clinical Practice Guidelines for diagnosis, treatment and follow-up. *Ann Oncol*. 2019;30(8):1194–1220.
61. Cardoso F, Costa A, Norton L, et al. ESO-ESMO 2nd international consensus guidelines for advanced breast cancer (ABC2). *Breast*. 2014;23(5):489–502.
62. Paluch-Shimon S, Pagani O, Partridge AH, et al. ESO-ESMO 3rd international consensus guidelines for breast cancer in young women (BCY3). *Breast*. 2017;35:203–217.
63. Paluch-Shimon S, Cardoso F, Partridge AH, et al. ESO-ESMO 4th international consensus guidelines for breast cancer in young women (BCY4). *Ann Oncol*. 2020;31(6):674–696.
64. Paluch-Shimon S, Cardoso F, Partridge AH, et al. ESO-ESMO fifth international consensus guidelines for breast cancer in young women (BCY5). *Ann Oncol*. 2022;33(11):1097–1118.
65. Partridge AH, Pagani O, Abulkhair O, et al. First international consensus guidelines for breast cancer in young women (BCY1). *Breast*. 2014;23(3):209–220.
66. Ohnstad HO, Borgen E, Falk RS, et al. Prognostic value of PAM50 and risk of recurrence score in patients with early-stage breast cancer with long-term follow-up. *Breast Cancer Res*. 2017;19(1):120.
67. Engstrøm MJ, Opdahl S, Hagen AI, et al. Molecular subtypes, histopathological grade and survival in a historic cohort of breast cancer patients. *Breast Cancer Res Treat*. 2013;140(3):463–473.
68. Gnant M, Filipits M, Greil R, et al. Predicting distant recurrence in receptor-positive breast cancer patients with limited clinicopathological risk: using the PAM50 Risk of Recurrence score in 1478 postmenopausal patients of the

ABCSG-8 trial treated with adjuvant endocrine therapy alone. *Ann Oncol*. 2014;25(2):339–345.
69. Dowsett M, Sestak I, Lopez-Knowles E, et al. Comparison of PAM50 risk of recurrence score with oncotype DX and IHC4 for predicting risk of distant recurrence after endocrine therapy. *J Clin Oncol*. 2013;31(22):2783–2790.
70. Lænkholm AV, Jensen MB, Eriksen JO, et al. PAM50 risk of recurrence score predicts 10-year distant recurrence in a comprehensive Danish cohort of postmenopausal women allocated to 5 years of endocrine therapy for hormone receptor-positive early breast cancer. *J Clin Oncol*. 2018;36(8):735–740.
71. Jensen MB, Lænkholm AV, Nielsen TO, et al. The Prosigna gene expression assay and responsiveness to adjuvant cyclophosphamide-based chemotherapy in premenopausal high-risk patients with breast cancer. *Breast Cancer Res*. 2018;20(1):79.
72. Lundgren C, Bendahl PO, Church SE, et al. PAM50 subtyping and ROR score add long-term prognostic information in premenopausal breast cancer patients. *NPJ Breast Cancer*. 2022;8(1):61.
73. Pan Y, Yu Y, Wang X, Zhang T. Tumor-associated macrophages in tumor immunity. *Front Immunol*. 2020;11:583084.
74. Martinez LM, Robila V, Clark NM, et al. Regulatory T cells control the switch from in situ to invasive breast cancer. *Front Immunol*. 2019;10:1942.
75. Qing T, Karn T, Rozenblit M, et al. Molecular differences between younger versus older ER-positive and HER2-negative breast cancers. *NPJ Breast Cancer*. 2022;8(1):119.
76. Pawelec G, Solana R. Immunosenescence. *Immunol Today*. 1997;18(11):514–516.
77. Montecino-Rodriguez E, Berent-Maoz B, Dorshkind K. Causes, consequences, and reversal of immune system aging. *J Clin Invest*. 2013;123(3):958–965.
78. Sun H, Huang W, Ji F, Pan Y, Yang L. Comparisons of metastatic patterns, survival outcomes and tumor immune microenvironment between young and non-young breast cancer patients. *Front Cell Dev Biol*. 2022;10,923371.
79. Bass BP, Engel KB, Greytak SR, Moore HM. A review of preanalytical factors affecting molecular, protein, and morphological analysis of formalin-fixed, paraffin-embedded (FFPE) tissue: how well do you know your FFPE specimen? *Arch Pathol Lab Med*. 2014;138(11):1520–1530.
80. Carithers LJ, Agarwal R, Guan P, et al. The biospecimen preanalytical variables program: a multiassay comparison of effects of delay to fixation and fixation duration on nucleic acid quality. *Arch Pathol Lab Med*. 2019;143(9):1106–1118.